JCEC
THE JOURNAL OF ENGINEERING AND EXACT SCIENCES

OPEN ACCESS

The Journal of Engineering and Exact Sciences – jCEC, Vol. 10 N. 03 (2024)
journal homepage: https://periodicos.ufv.br/jcec
eISSN: 2527-1075
ISSN: 2446-9416

Numerical Investigation of Bearing Capacity of Centrally and Eccentrically Loaded Surface Footing on Sand-Clay with Void Using Plaxis 2D

Article Info:
Article history: Received 2024-01-11 / Accepted 2024-04-14 / Available online 2024-04-14
doi: 10.18540/jcecvl10iss3pp17506

Abdelhakim Nezari
ORCID: https://orcid.org/ 0009-0005-4402-4471
Laboratory of Applied Civil Engineering (LGCA), Department of Civil Engineering, Echahid Cheikh Larbi Tebessi University, Algeria
E-mail: abdelhakim.nezari@univ-tebessa.dz
Rafik Boufarh
ORCID: https://orcid.org/ 0000-0002-1793-2950
Laboratory of Applied Civil Engineering (LGCA), Department of Civil Engineering, Echahid Cheikh Larbi Tebessi University, Algeria
E-mail: rafik.boufarh@univ-tebessa.dz
Tarek Mansouri
ORCID: https://orcid.org/ 0000-0002-1793-2950
Laboratory of Applied Civil Engineering (LGCA), Department of Civil Engineering, University of Batna 2, Algeria
E-mail: t.mansouri@univ-batna2.dz

Abstract
The presence of voids under footings can significantly reduce the stability of the foundation and the superstructure above it. Estimating the bearing capacity of a footing with voids below it is a complex and challenging problem in geotechnical engineering. This study investigates the stability of centrally and eccentrically loaded surface footings supported by sand layers of variable thickness overlying clay layers, with circular voids below the center of the footing. Using the Plaxis finite element software, the influence of various parameters on the overall performance of the footing, including load eccentricity, void location, void size, and introducing geogrid reinforcement at the sand-clay interface are analyzed. The results show that increasing the void depth, add a thick layer of sand or introducing geogrid reinforcement can mitigate the impact of a void beneath a foundation.
Keywords: bearing capacity. eccentricity. sand overlying clay. strip footings. reinforced soils. Void.

1. Introduction

In engineering practice, underground voids are often found under the footings of buildings. These voids can be formed naturally, such as by the dissolution of gypsum or the leakage of CO2 from a storage tank, or they can be man-made, such as by the excavation of mines, pipe tunnels, or basements. The presence of voids under footings can have a significant impact on the stability of the foundation and the superstructure it supports. The accurate estimation of the bearing capacity of a footing with underlying voids is one of the most complex and challenging problems in geotechnical engineering.

Most previous studies have focused on analyzing man-made voids. For example, the researches of Baus and Wang (1983) and Badie and Wang (1984) found that there is a critical area

under the footing where the footing's performance is most affected. Wang and Badie (1985) further investigated the effects of different parameters, such as the shape of the footing (square or strip), the shape of the void (continuous circular or cubic), the orientation of the voids with respect to the footing (parallel or perpendicular), and the location of the voids. Their findings suggest that the subsurface hole will only compromise the footing's stability if it is located above a critical depth.

In a study of the stability of footings on layered deposits with and without voids, Azam *et al*. (1991) found that the thickness of the top layer and the strength ratio between the two layers affect the performance of the footing. They also found that the introduction of a geogrille nappe at the sand-clay interface can further increase the bearing capacity of the soil. This method of reinforcement is widely used in geotechnical engineering and has been the subject of extensive theoretical and experimental research. The following studies can be cited: (Briançon & Villard, 2006; Khing *et al*., 1994; Love *et al*., 1987; Villard *et al*., 2002). In this technique, the beneficial effects of reinforcement are derived from the action of the membrane, which requires a high allowable depth.

In practice, eccentric loads on footings are often expressed as the ratio of the moment (M) to the vertical load (Q). Most footings are subjected to moments caused by lateral forces acting on the superstructure, such as earthquakes, lateral soil pressures, water, wind, braking forces, and so on. However, most research has focused on vertically centered loading on footings. A few studies have investigated eccentrically loaded footings, but they are not well-cited (El Sawwaf, 2009; Moroglu *et al*., 2005; Sadoglu *et al*., 2009; Sahu *et al*., 2016). These studies found that the eccentricity of the loads changes the failure modes of the system and the bearing capacity of the footing/void system.

Recently, a significant amount of research has been published on the stability of footings when the effects of voids and eccentric loads are combined (Mansouri *et al*., 2021; Wu, Zhao, Zhang, *et al*., 2020; Wu, Zhao, Zhao, *et al*., 2020). Mazouz *et al*. (2022) conducted a study on the load-bearing capacity of a strip footing placed on an unreinforced and geogrid-reinforced sand slope with a circular void subjected to a vertical static load. They investigated the effects of various parameters, such as the number of geogrid layers (N), the ratio of the vertical distance between the top of the void and the base of the footing (H/B), the horizontal distance of the void axis from the base of the footing (H/B), and the horizontal distance between the center of the void and the center of the footing (X/B). The results showed that there is a critical zone under the footing where the existence of voids has no effect on the load-bearing capacity and stability of the footing. Additionally, the use of geogrid reinforcement reduces settlement and improves bearing capacity. Finally, the bearing capacity factor and failure mechanism increase with increasing horizontal and vertical distance ratios between the voids (X/B and H/B) and reinforcement layers.

This paper presents finite element analyses using Plaxis 2D to calculate the bearing capacity of a surface footing centrally and eccentrically loaded, supported by a stronger sand layer of variable thickness H, overlying a weaker clay, with a continuous circular void located below the center of the foundation (Fig. 1). Numerical simulations were carried out with and without a geogrid layer. The overall objective of this study is to assess the influence of various parameters such as load eccentricity, void location, and void size on the overall performance of the footing. Then to improve its bearing capacity by introducing geogrid reinforcement at the sand-clay interface, the details of which are presented later in this study.

2. Problem definition

Figure 1 shows the main parameters used in this investigation. An eccentrically loaded footing of width B is resting on a weaker clay layer and supported by a stronger sand layer of limited thickness H. The footing has a continuous circular void underneath its center. The dimensionless width of the void is defined as D/B. The vertical distance between the void and the upper limit of the clay layer is d/B, and the dimensionless vertical distance of the sand layer is H/B.

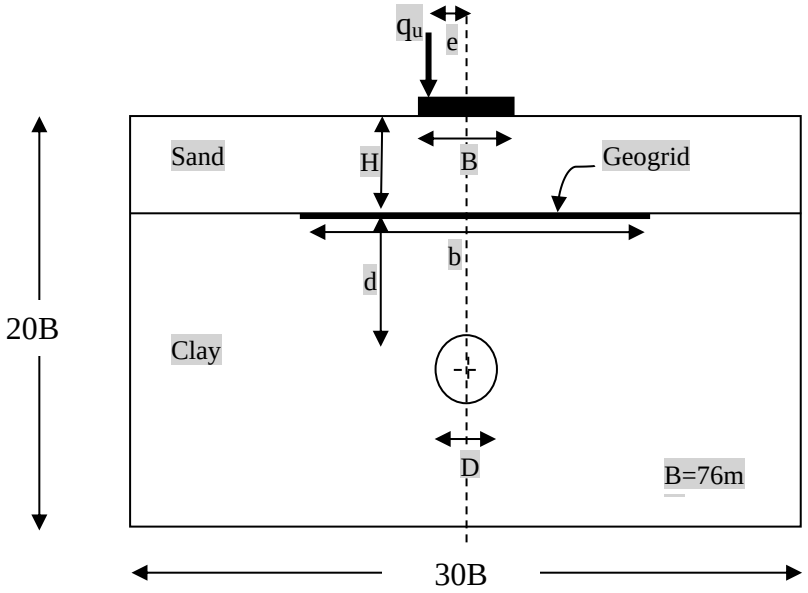

Figure 1 - Overview of the problem.

A concentrated load is applied to the rigid footing, and the dimensionless distance between the center point of the footing and the load is defined as e/B. Due to symmetry, only the left eccentric load is considered. Finally, to further improve the bearing capacity of the foundation, a layer of geogrid with width b=6B is placed at the sand-clay interface.

Table 1 presents the test program of this study, which consisted of four series of tests to analyze the combined effect of several parameters on the bearing capacity of surface foundations supported by a bi-layer containing a void. Figure 1 illustrate the different tests conducted in this study, with the details of the parameters. Each series of tests aimed to analyze the combined effect of two parameters, while the other parameters were kept constant.

Series 1 investigated the effect of the sand layer thickness (H/B) with different loading cases (e/B), while Series 2 investigated the same parameters with the addition of a geogrid layer at the sand-clay interface. The variable parameters in Series 3 included the depth from the upper boundary of the clay layer to the top of the cavity (d/B), the width of the subsurface void (D/B), and the different loading cases (centered and eccentric). Series 4, which consisted of 80 tests, included the same variable parameters as Series 3, with the exception of a geogrid reinforcement layer introduced at the contact surface between the sand and the clay.

Table 1 - Tests program.

Serie	*b/B*	*H/B*	D/B	d/B	*e/B*	remarks
1	0	0 0.5 1 1.5 2 3	0	/	0, 0.1, 0.2, 0.3 0, 0.1, 0.2, 0.3 0, 0.1, 0.2, 0.3 0, 0.1, 0.2, 0.3 0, 0.1, 0.2, 0.3 0, 0.1, 0.2, 0.3	Tests without void and without geogrid at sand-clay interface
2	6	0 0.5 1 1.5 2 3	0	/	0, 0.1, 0.2, 0.3 0, 0.1, 0.2, 0.3 0, 0.1, 0.2, 0.3 0, 0.1, 0.2, 0.3 0, 0.1, 0.2, 0.3 0, 0.1, 0.2, 0.3	Tests without void and with geogrid at sand-clay interface
3	0	H/B that gives maximum ultimate bearing capacity	0.5 1 1.5 2	0.5 1 1.5 2 3	0, 0.1, 0.2, 0.3 0, 0.1, 0.2, 0.3 0, 0.1, 0.2, 0.3 0, 0.1, 0.2, 0.3 0, 0.1, 0.2, 0.3	Tests with void and without geogrid at sand-clay interface
4	6	H/B that gives maximum ultimate bearing capacity	0.5, 1, 1.5, 2	0.5, 1, 1.5, 2, 3	0, 0.1, 0.2, 0.3	Tests with void and with geogrid at sand-clay interface

3. Finite element model

Two-dimensional finite element calculations were performed using Plaxis 2D, a robust and user-friendly software program that has been increasingly used in recent years to assess soil deformation and stability. The geogrid was modeled using 5-node elastic elements, the soil was modeled using 15-node triangular elements, and the footing was modeled using 6-node triangular plate elements. Figure 2 shows the boundary conditions and finite element mesh used in this study. The boundary limits were placed below ground level and more than 12B laterally from the edge of the foundation to minimize the effects of the boundaries on the estimated load capacity. Zero horizontal displacements were specified at the lateral boundaries, and full fixities were specified at

the base. Excavating the soil to the required depth for each analysis resulted in the introduction of voids.

The mesh density in the vicinity of the footing, the geogrid layer, and the void is crucial for determining the load capacity. To ensure a better representation of the stress field and to increase the precision of the results, the refined mesh option was chosen in these areas. The soil is considered to be an elastic, perfectly plastic material that conforms to the non-associated flow rule and the Mohr-Coulomb criterion. This is more accurate for the thick sand layer than for the surrounding soft clay layer. The secant Young's modulus (E), Poisson's ratio (ν), effective cohesion (c), internal friction angle (φ), and dilation angle (ψ) are used to define the stress limit state. Table 2 summarizes the parameters used for the analysis.

According to the Mindlin beam theory (Mindlin, 1951), the footing is modeled as a rigid frame with significant bending rigidity (EI) and normal rigidity (EA). The geostatic stress was generated by applying the coefficient at rest earth pressure, $K_0 = 1\text{-}\sin\varphi$. The void is modeled as an unlined tunnel and is considered to be round with a variable dimensionless width D/B.

According to (Khing *et al.*, 1994), the reinforcement layer added at the sand/clay interface is often used to enhance the bearing capacity. This reinforcement layer is simulated using Plaxis' elastic geogrid element option, with EA = 182 kN/m. In all cases of loading, centered or eccentric, the footing reaches a clear collapse load, which is taken as the maximum load of the load-displacement behavior.

Table 2 - Finite element analysis parameters.

Parameter	index	Unit	Dense sand	Soft clay	Footing	Geogrid
Cohesion	c	kN/m^2	1	11.8		
Friction angle	φ	(°)	40.3	1		
Dilatancy angle	ψ	(°)	10			
Dry density	γ_{unsat}	KN/m^3	17.14	15.5		
Wet density	γ_{sat}	KN/m^3	18	18.1		
Poisson's ratio	ν		0.25	0.3		
Young's modulus	E_{ref}	kN/m^2	100 000	10 000		
EA of the footing	EA	kN/m			$5.00x10^9$	
EI of the footing	EI	kN m^2/m			$8.50x10^9$	
EA of the geogrid	EA	kN/m				182

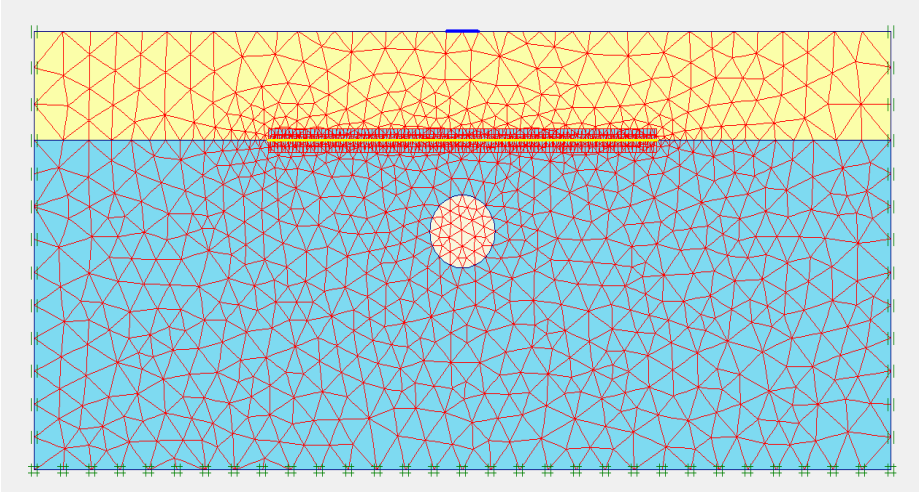

Figure 2 - Boundary conditions and finite element mesh used in this study.

4. The finite element model's validation

To validate the established model's accuracy, the bearing capacity of a strip footing resting on a void-free sand layer overlying clay was simulated using Plaxis 2D. The obtained results were then compared to those from previous studies in the literature. This comparison included Burd and Frydman (1996)'s finite element method-based results, Michalowski and Shi (1995)'s upper-bound limit analysis-based results, Shiau *et al*. (2003)'s finite element method of limit analysis theorems-based results, and Chaabani *et al*. (2022) finite difference method-based results. Figure 3 depicts the normalized bearing capacity qu/γB as a function of the normalized undrained shear strength of clay (Cu/γB) for a thickness-to-width ratio (H/B) of 1 and friction angles (φ) of 40° for sand. As shown in Figure 3, there is a good correlation between the ultimate bearing capacity of the numerical model and those previously reported. This correlation supports the validation of the numerical model.

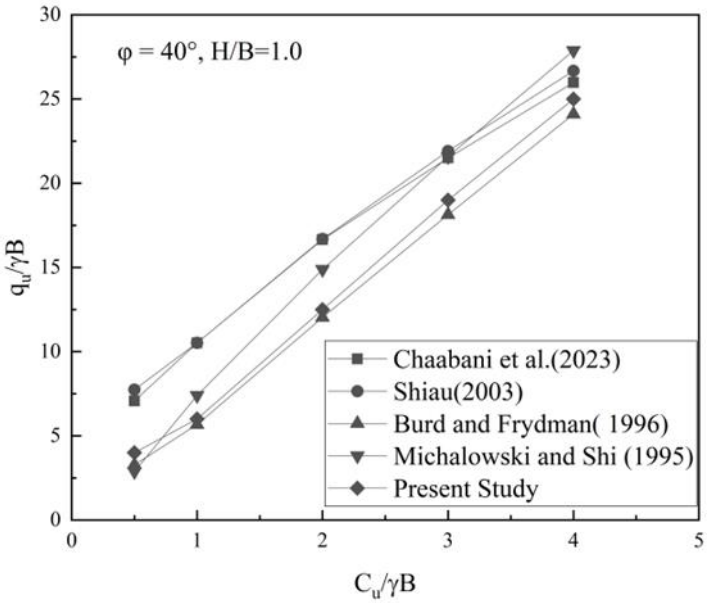

Figure 3 - Dimensionless Bearing Capacity ($q_u/\gamma B$) for Varying $c_u/\gamma B$ Values Compared with Literature Results (φ = 40°, H/B = 1).

5. Results and discussion

To investigate the effect of cavity size (D/B) and position (d/B) on loading eccentricity, four (4) test series with a total of 208 tests were conducted. A strip footing of width B with a range of eccentric vertical load ratios (e/B = 0, 0.1, 0.2, and 0.3) was supported by a more resistant sand layer of limited thickness H, resting on a weaker clay, with a continuous circular void located below the center of the foundation. The cavity size (D/B) varied from 0.5 to 2, and the cavity position (d/B) varied from 0.5 to 3. A simplified validation test with a centered load, a single clay layer, and no void was also conducted to assess the reliability of the test results. The bearing capacity was determined by dividing the limit load by the footing surface area. The load capacity calculation results were obtained using the tangent intersection method. A layer of geogrid (b = 6B) was placed at the sand-clay interface to further increase the foundation's bearing capacity.

5.1. Effect of Sand Layer Thickness

Two series of curves showing the ultimate bearing capacity as a function of sand layer thickness have been plotted based on the results of Series I and II tests (without and with geogrid, respectively), for both centered and eccentric loads.

Figure 4 shows that the bearing capacity increases with the thickness of the sand layer, reaching a maximum value at H/B = 3. Beyond this value, the bearing capacity remains approximately constant. When H/B is sufficiently large, the failure surface is completely contained within the sand layer. The eccentricity of the loading reduces the bearing capacity. Additionally, the inclusion of a geogrid layer significantly improves the bearing capacity, especially in the range H/B = 1 to 1.5 (see Figure 5). This finding confirms the results of the work of Khing *et al*. (1994). However, the influence of the geogrid layer is negligible for H/B ≥ 3.

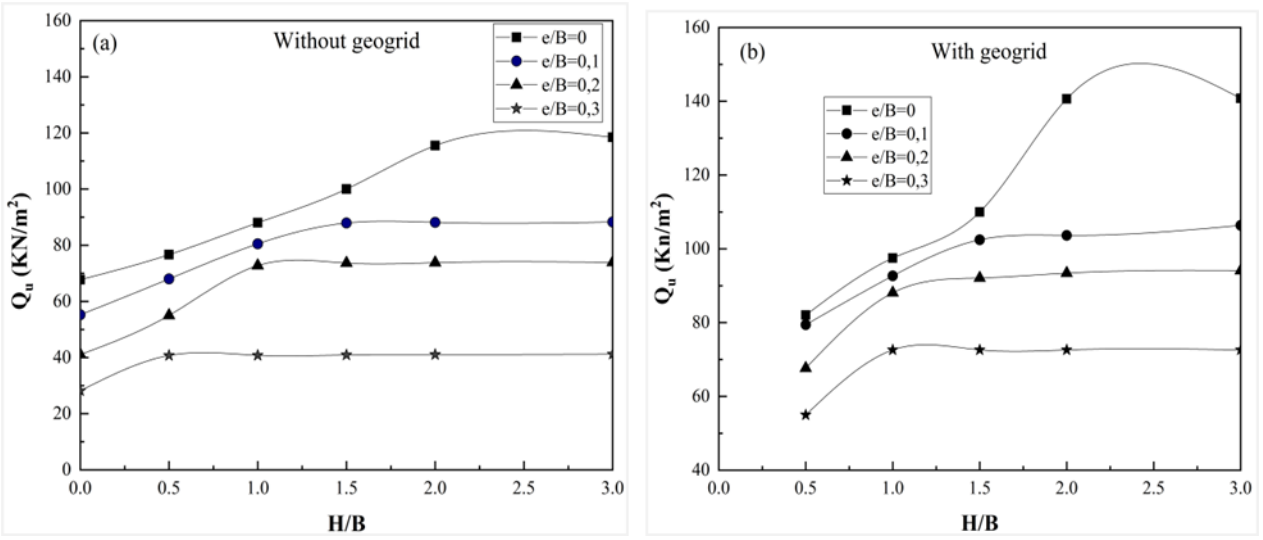

Figure 4 - Variation in ultimate bearing capacity as a function of H/B
a) Without geogrid reinforcement, b) With geogrid reinforcement

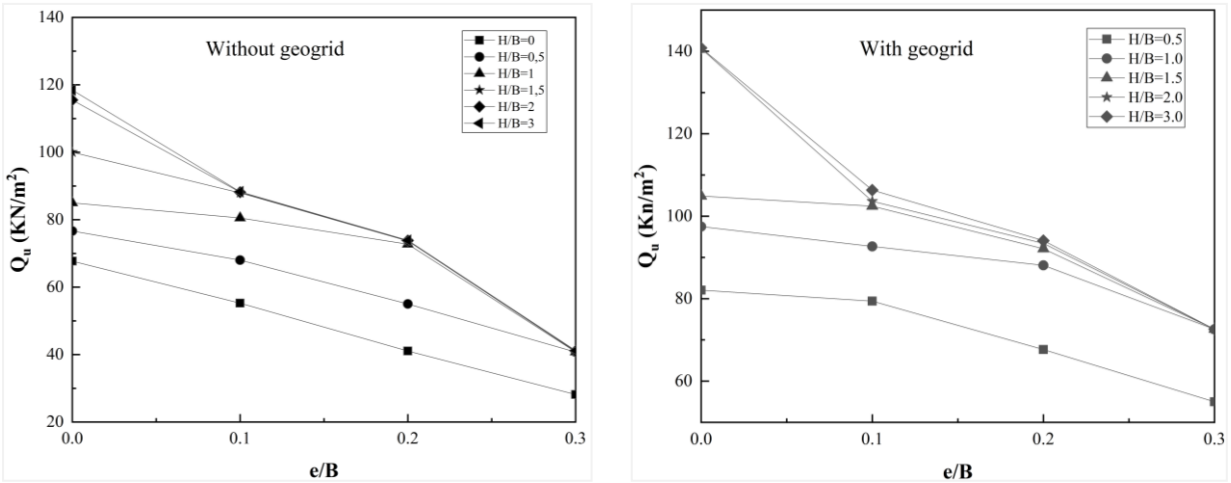

Figure 5 - Bearing capacity variation as a function of thickness ratio H/B (series I and II)

The variation in bearing capacity efficiency as a function of eccentricity e/B can be described as follows in order to achieve this goal and to illustrate the effect of eccentric loading:

$$\eta = \frac{qu\ (e/B\neq 0)}{qu\ (e/B=0)} \quad \text{(without geogrid)} \quad (1)$$

$$\eta_{reinforced} = \frac{qu-\ reinforced(e/B\neq 0)}{qu-reinforced\ (e/B=0)} \quad \text{(with geogrid)} \quad (2)$$

According to Figure 6, for a given value of eccentricity, the η ratio decreases with decreasing H/B. For H/B = 0 (without sand layer), η and $\eta_{reinforced}$ decrease from 100% for e/B = 0 to around 40% for e/B = 0.3, a drop of 60%. Similarly, for H/B = 3, η and $\eta_{reinforced}$ decrease from 100% for e/B = 0 to around 75% for e/B = 0.3, a reduction of only 25%. The H/B = 3 case shows no effect from geogrid reinforcement, confirming the previous finding that the influence of geogrid reinforcement is negligible for H/B ≥ 3. Therefore, as a conclusion, the sand layer is dominant over the geogrid layer, regardless of the type of loading applied (centric or eccentric).

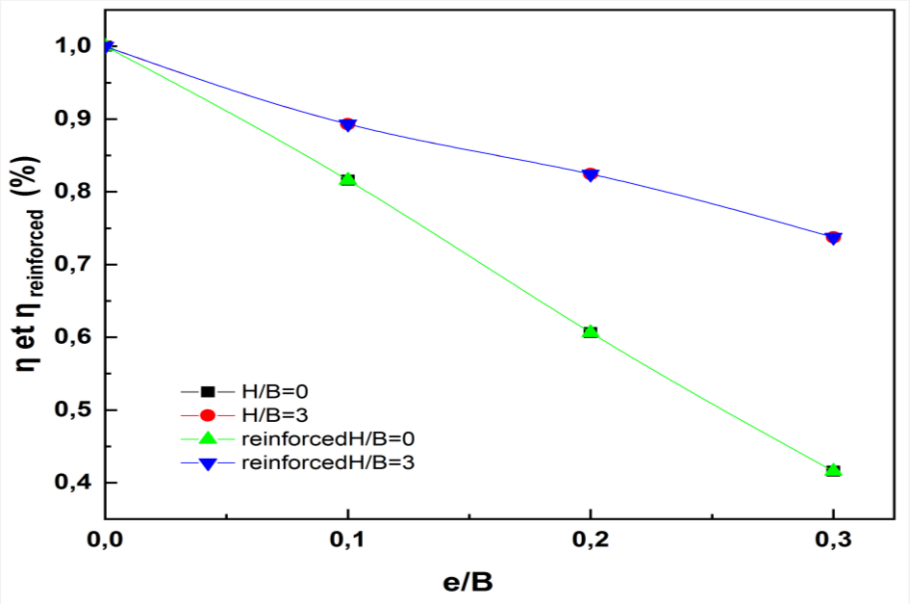

Figure 6 - Variation of η and $\eta_{reinforced}$ with e/B (Series I and II)

5.2. *Effect of Cavity Depth*.

To better visualize the effect of the depth of the underground void beneath the foundation, a series of curves for the bearing capacity factors Ω_d and $\Omega_{d\text{-reinforced}}$ as a function of depth d/B and different void diameters have been plotted for the case of a centered load (e/B = 0) only. This is because Ω_d can be given in the form given in Equation (3), where it is defined as the ratio between the bearing capacity in which a void was present beneath the foundation and the bearing capacity of the footing without a subsurface void.

$$\Omega_d = \frac{q_u-\text{with void}}{q_u-\text{without void}} \quad (3)$$

Whereas the second factor $\Omega_{d\text{-reinforced}}$ (equation 4) is defined as the ratio between the bearing capacity of a reinforced foundation over a void and that reinforced without a void.

$$\Omega_{d-reinforced} = \frac{q_{u-reinforced}\ \text{with void}}{q_{u-reinforced}\ \text{without void}} \quad (4)$$

Figures 7 and 8 show the variation of the factors Ω_d and $\Omega_{d\text{-reinforced}}$ with the void depth ratio (d/B) from 0.50 to 3. Both factors increase continuously with increasing depth ratio up to a critical value of d/B = 3, beyond which they remain stable. This means that the footing converges towards the void-free case. The same conclusion was reached in Das and Khing (1994).

One exception is shown in Figure 7 for the case D/B = 2, where the critical depth ratio is greater than 3 (d/B > 3) due to the size of the cavity. Figure 9 also shows that the introduction of the geogrid increases the bearing capacity ratio regardless of the void depth and for all void diameters. This increase is around 2% for D/B = 0.5 and d/B = 0.5, and around 5% for D/B = 2 and d/B = 0.5. Additionally, for a given d/B ratio, the factors Ω_d and $\Omega_{d\text{-reinforced}}$ decrease with increasing D/B ratio. For D/B = 0.5, Ωd and Ωd-reinforced increase from 94% for d/B = 0.5 to 100% for d/B ≥ 2. Similarly, for D/B = 2 (worst case), Ωd and Ωd-reinforced increase from 63% for d/B = 0.5 to around 93% for d/B = 3.

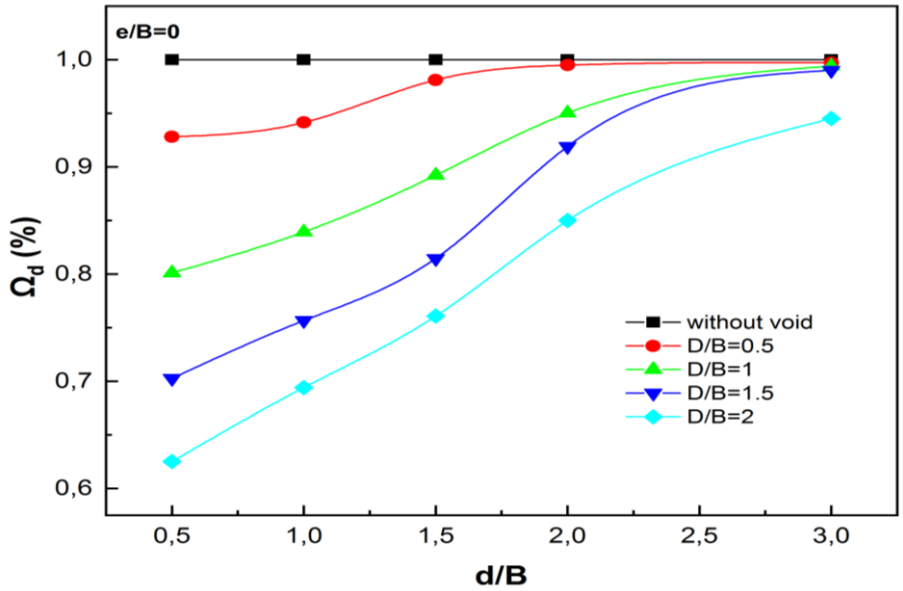

Figure 7 - Variation of Ω_d as a function of d/B (series I and III)

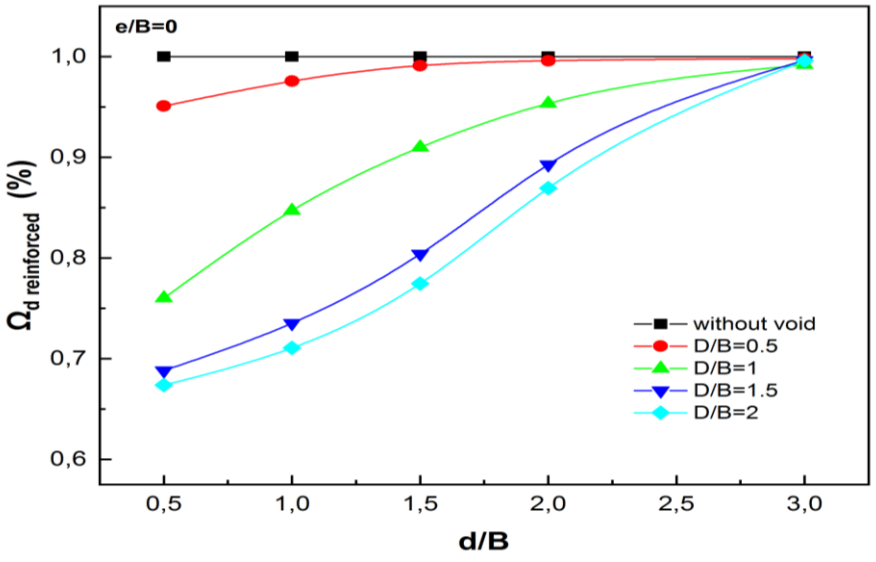

Figure 8- Variation of $\Omega_{d\text{-reinforced}}$ as a function of d/B (series II and IV)

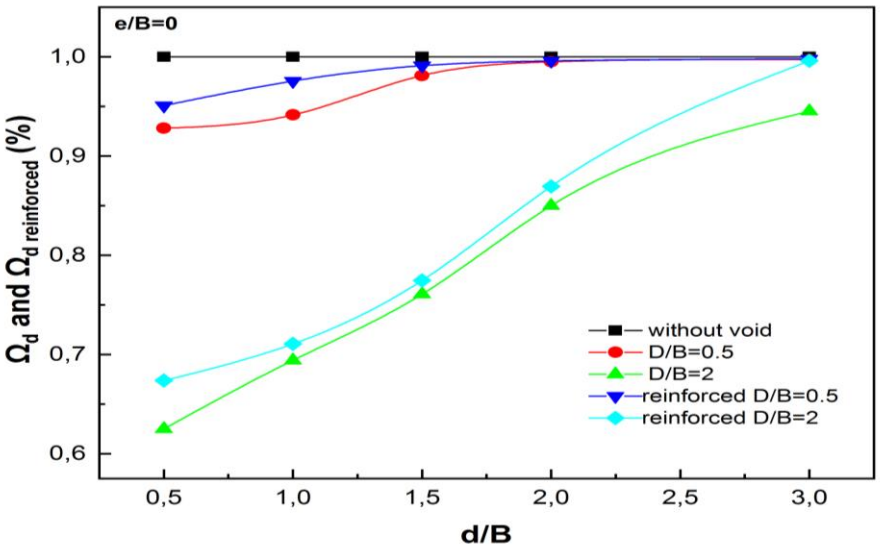

Figure 9 - Variation of Ω_d and $\Omega_{d\text{-reinforced}}$ as a function of d/B (series I, II, III and IV)

5.3. Cavity Size Effect.

As a function of cavity diameter D/B and under a centered load, the variation of the ultimate load-bearing capacity ratio can be noted as follows:

$$\Omega_D = \frac{q_u - \text{with void}}{q_u - \text{without void}} \quad (5)$$

$$\Omega_{D-\text{reinforced}} = \frac{q_{u-reinforced}\ \text{with void}}{q_{u-reinforced}\ \text{without void}} \quad (6)$$

q_u with void and q_u without void, respectively, describe the unreinforced bearing capacities of the soil with and without void, while $q_{\text{u-reinforced}}$ with void and $q_{u-reinforced}$ without void define the reinforced case.

Figures 10 and 11 show the variation of the factors Ω_D and $\Omega_{D\text{-reinforced}}$ as a function of the diameter ratio (D/B). Due to the rise in void diameter, the load-bearing capacity ratio decreases significantly with increasing void diameter. However, for the case d/B = 3, the bearing capacity ratio remains constant, regardless of the diameter of the underground void. This exception can be explained by the fact that at this depth, the behavior is the same as the case without a void.

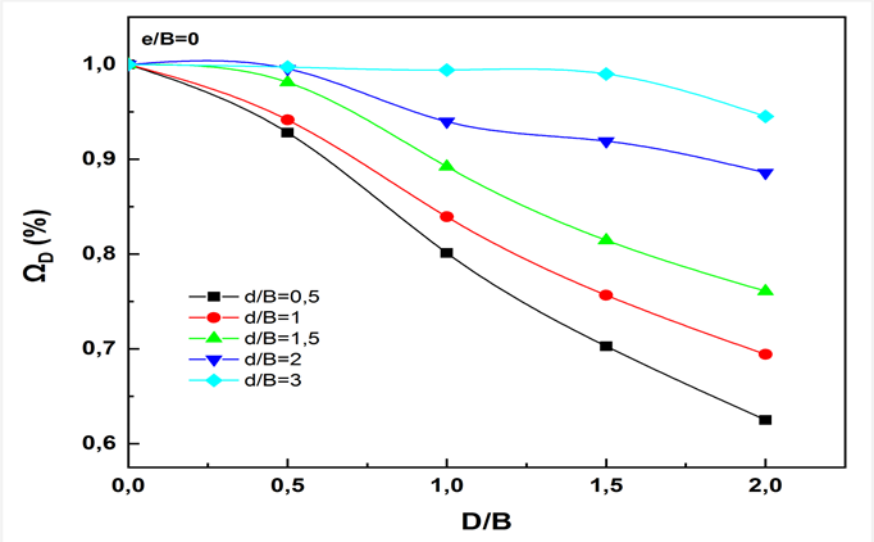

Figure 10 - Variation of Ω_D as a function of D/B (series I and III)

The obtained results confirm that bearing capacity ratios generally decrease with the presence of a void beneath the foundation. For a given void depth, the variation in bearing capacity as a function of D/B for the reinforced and unreinforced cases is practically the same (Figure 12), except for the cases D/B = 2 and d/B = 3. In these cases, the introduction of a layer of geogrid at the sand-clay interface has a beneficial effect, with a gain of around 5%.

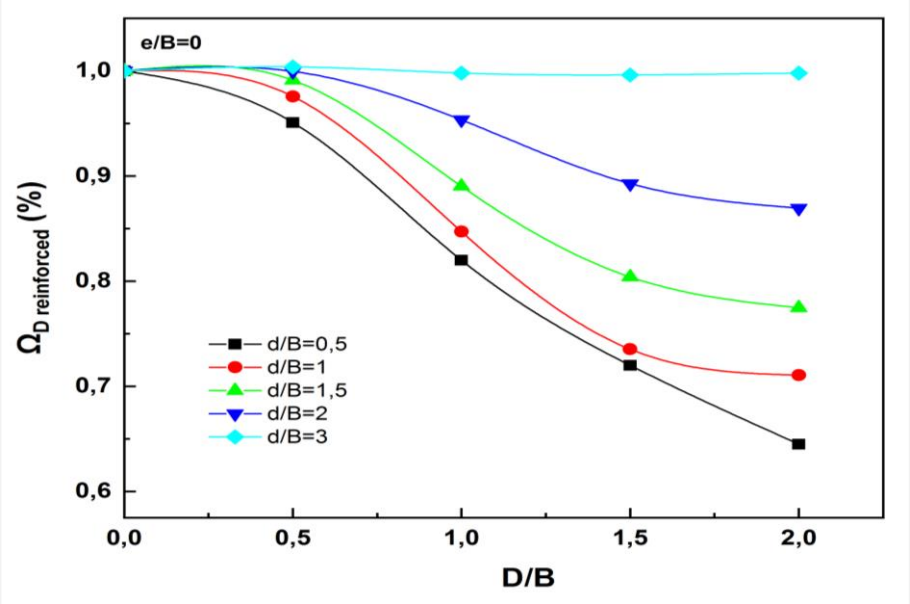

Figure 11- Variation of $\Omega_{D\text{-reinforced}}$ as a function of D/B (series II and IV)

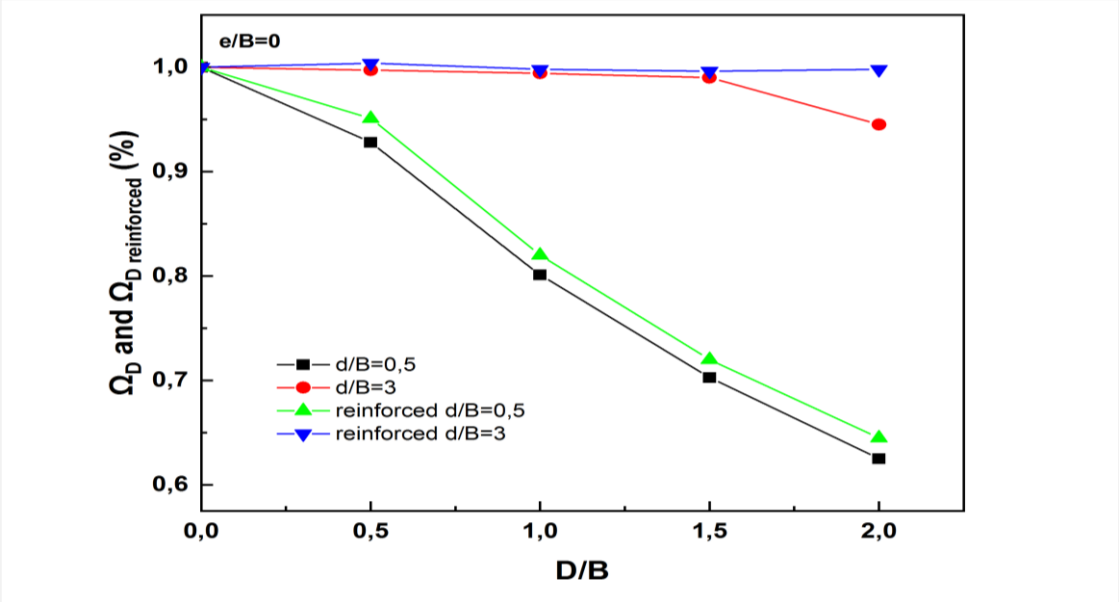

Figure 12- Variation of Ω_D and $\Omega_{D\text{-reinforced}}$ as a function of D/B (series I, II, III and IV)

5.4. Eccentric loading's effects.

A series of curves have been plotted to show how the bearing capacity factors change as a function of the eccentricity ratio (e/B), allowing for a more comprehensive examination of the impact of eccentric loading on the bearing capacity of a shallow foundation over a circular void.

In Figures 13 and 14, the change of η_e and $\eta_{e\text{-}R}$ is shown in relation to eccentricity (e/B), various void diameters (D/B), and the critical depth (d/B = 3). The ratio between the bearing

capacities of an eccentrically loaded foundation and a footing with a centric load is denoted by the symbol ηe in Equation (7).

$$\eta_e = \frac{qu\ (e/B\neq 0)}{qu\ (e/B=0)} \qquad \text{without geogrid} \qquad (7)$$

$\eta_{e\text{-}R}$ given in equation (8) is defined as the ratio between the bearing capacity of an eccentrically loaded reinforced foundation over a void and that reinforced with a centric load.

$$\eta_{e-R} = \frac{qu-R(e/B\neq 0)}{qu-R\ (e/B=0)} \qquad \text{With geogrid} \qquad (8)$$

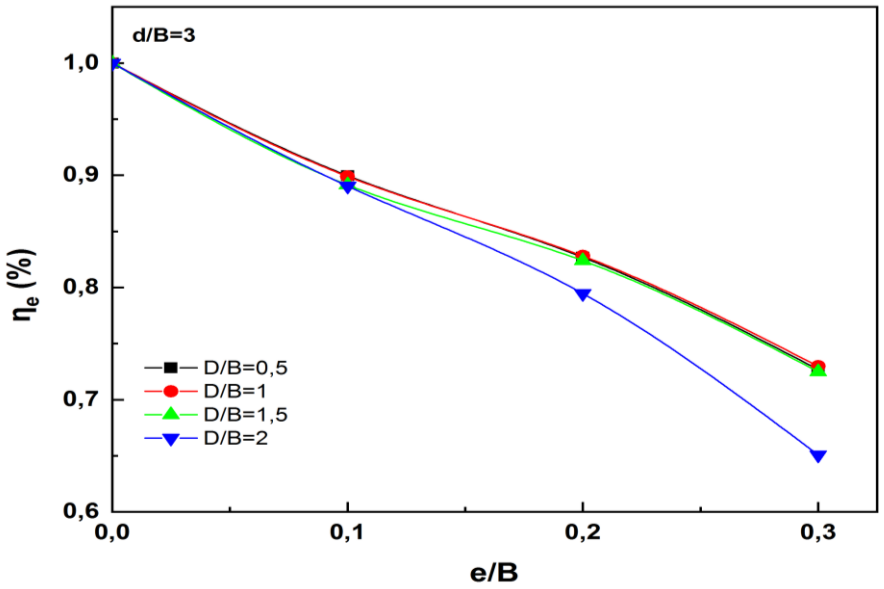

Figure 13 - Variation of η_e as a function of e/B (serie III)

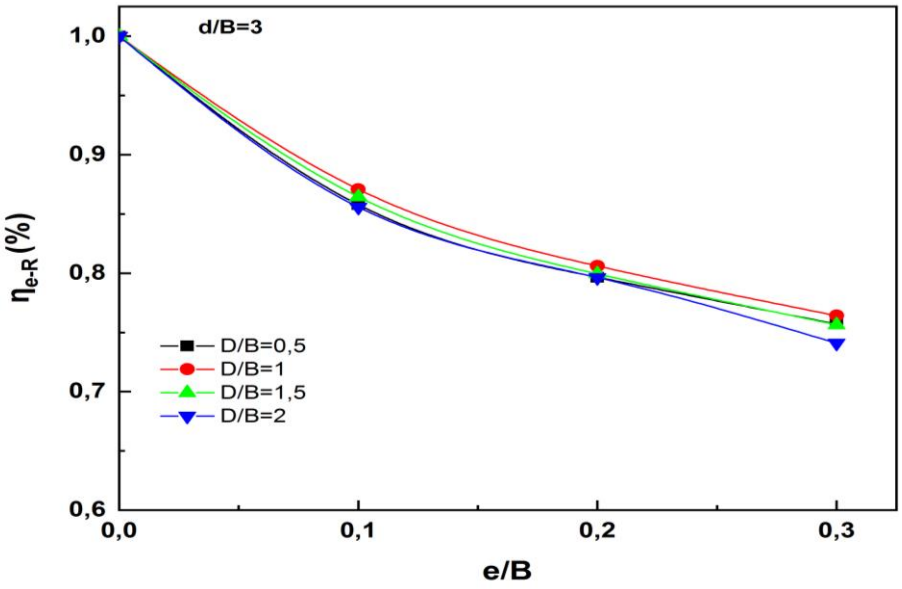

Figure 14 - Variation of $\eta_{e\text{-}R}$ as a function de e/B (serie IV)

For a given value of eccentricity, the ratios η_e and $\eta_{e\text{-}R}$ are almost identical for different void sizes ranging from 0.5 to 2, except for the D/B = 2 case, where the ratios decrease with increasing void size. This similarity of the curves confirms that there is no significant influence of void size for a depth d/B = 3 (critical depth). The only significant influence is that of eccentric loading, with

a regression rate of 25%, as previously observed for the no-void case in Figure 5. This indicates that the ultimate load capacities of eccentrically loaded continuous footings decrease with increasing eccentricity. On the other hand, the divergence of the D/B = 2 curve from the other curves confirms the influence of void size. This is because the ratios η_e and $\eta_{e\text{-}R}$ decrease further, proportional to the increase in eccentricity. For the unreinforced case, the decrease is estimated to be 4% for e/B = 0.2 and around 8% for e/B = 0.3.

For the reinforced case, the decrease is estimated to be around 3% for e/B = 0.3. This leads us to conclude that the interference effect becomes more pronounced as the void size ratio and eccentricity increase. Therefore, adding a layer of geogrid at the sand-clay interface is beneficial (by around 5%) for the given case of D/B = 2 at a critical depth of d/B = 3.

6. Conclusions

A numerical study was conducted to investigate the stability of surface footing centrally and eccentrically loaded, supported by a stronger sand layer of variable thickness H, overlying a weaker clay, with a continuous circular void located below the center of the foundation. Using the Plaxis finite element software, the ultimate bearing capacity of the strip footing has been calculated with and without a geogrid layer. Furthermore, the effects of load eccentricity, location and size of void on the overall performance of the footing were studied, alongside an examination of the effect of reinforcement.

The results of this study suggest that the ultimate bearing capacity is affected by the aforementioned parameters. Based on these findings, we can draw the following conclusions:

- The reinforcement and thickness of the sand layer are significant parameters that influence the ultimate bearing capacity of a strip footing on sand overlying clay without a void. In fact, increasing these two parameters significantly improved the ultimate bearing capacity.
- The H/B = 3 case shows no effect from geogrid reinforcement, confirming the previous finding that the influence of geogrid reinforcement is negligible for $H/B \geq 3$. This suggests that the sand layer is dominant over the geogrid layer, regardless of the type of loading applied (centric or eccentric). In other words, for $H/B \geq 3$, the geogrid reinforcement has no significant impact on the bearing capacity of the sand layer. This is because the sand layer is thick enough to provide adequate support for the load, and the geogrid is not able to provide any additional reinforcement.
- The behavior of a footing with a void in its failure zone is significantly affected, reducing its ultimate bearing capacity and stability.
- The introduction of a geogrid reinforcement can increase the bearing capacity ratio of a footing with a void, regardless of the void depth and diameter. The increase is around 2% for a small void (D/B = 0.5) and a small void depth (d/B = 0.5), and around 5% for a large void (D/B = 2) and a small void depth (d/B = 0.5). Additionally, for a given void depth ratio, the bearing capacity ratio decreases with increasing void diameter. One exception for the case D/B = 2, where the critical void depth ratio (the depth at which the bearing capacity ratio reaches a stable value) is greater than 3 (d/B > 3) due to the large size of the cavity.
- The bearing capacity ratio of a footing with a void decrease significantly with increasing void diameter, except for the case where the void depth ratio is equal to 3. At this embedding distance, the behavior of the footing is the same as the case without a void, and the bearing capacity ratio remains constant. However, for a given void depth, the variation in bearing capacity as a function of void diameter is practically the same for the reinforced and unreinforced cases, except for the cases where the void diameter is equal to 2 and the void depth ratio is equal to 0.5. In these cases, the introduction of a geogrid reinforcement at the sand-clay interface can increase the bearing capacity ratio by up to 5%.
- Overall, the results of this study suggest that the presence of a void beneath a foundation can have a significant impact on its bearing capacity. However, the impact can be mitigated by increasing the void depth or by introducing a geogrid reinforcement.

- For a given value of eccentricity, the bearing ratios of eccentrically loaded continuous footings with voids at a critical depth (d/B = 3) are almost identical for different void sizes ranging from 0.5 to 2, except for the case D/B = 2, where the ratios decrease with increasing void size. This indicates that the ultimate load capacities of eccentrically loaded continuous footings with voids at a critical depth decrease with increasing eccentricity, and that the influence of void size is only significant for the case D/B = 2.

One way to further improve the performance of eccentrically loaded continuous footings with voids is to use a combination of void depth, add a thick layer of sand and geogrid reinforcement. For example, for a case where the void diameter is large and the critical void depth ratio is greater than the actual void depth ratio, the introduction of a geogrid reinforcement could help to increase the bearing capacity ratio by more than 5%.

Acknowledgements

This research was supported by Algeria's Directorate- General for Scientific Research and Technological Development (DGRSDT). The authors express special thanks to the University of Echahid Cheikh Larbi Tebessi and the laboratory of Applied Civil Engineering (LGCA). Any opinions, findings, conclusions, or recommendations expressed in this publication are those of the authors.

References

Azam, G., Hsieh, C., & Wang, M. (1991). Performance of strip footing on stratified soil deposit with void. *Journal of Geotechnical Engineering*, *117*(5), 753-772.

Badie, A., & Wang, M. (1984). Stability of spread footing above void in clay. *Journal of Geotechnical Engineering*, *110*(11), 1591-1605.

Baus, R., & Wang, M. (1983). Bearing capacity of strip footing above void. *Journal of Geotechnical Engineering*, *109*(1), 1-14.

Briançon, L., & Villard, P. (2006). Dimensionnement des renforcements géosynthétiques de plates-formes sur cavités. *Revue française de géotechnique*(117), 51-61.

Burd, H. J., & Frydman, S. (1996). Discussion of "Bearing capacity of footings over two-layer foundation soils" by Radoslaw L. Michalowski and Lei Shi. *Journal of Geotechnical Engineering*, *122*(8), 699-700.

Chaabani, W., Remadna, M. S., & Abu-Farsakh, M. (2022). Numerical modeling of the ultimate bearing capacity of strip footings on reinforced sand layer overlying clay with voids. *Infrastructures*, *8*(1), 3.

El Sawwaf, M. (2009). Experimental and numerical study of eccentrically loaded strip footings resting on reinforced sand. *Journal of Geotechnical and Geoenvironmental Engineering*, *135*(10), 1509-1518.

Khing, K., Das, B., Puri, V., Yen, S., & Cook, E. (1994). Foundation on strong sand underlain by weak clay with geogrid at the interface. *Geotextiles and Geomembranes*, *13*(3), 199-206.

Love, J., Burd, H., Milligan, G., & Houlsby, G. (1987). Analytical and model studies of reinforcement of a layer of granular fill on a soft clay subgrade. *Canadian Geotechnical Journal*, *24*(4), 611-622.

Mansouri, T., Boufarh, R., & Saadi, D. (2021). Effects of underground circular void on strip footing laid on the edge of a cohesionless slope under eccentric loads. *Soils and Rocks*, *44*.

Mazouz, B., Mansouri, T., Baazouzi, M., & Abbeche, K. (2022). Assessing the Effect of Underground Void on Strip Footing Sitting on a Reinforced Sand Slope with Numerical Modeling. *Engineering, Technology & Applied Science Research*, *12*(4), 9005-9011.

Michalowski, R. L., & Shi, L. (1995). Bearing capacity of footings over two-layer foundation soils. *Journal of Geotechnical Engineering*, *121*(5), 421-428.

Mindlin, R. (1951). Influence of rotatory inertia and shear on flexural motions of isotropic, elastic plates. *Journal of Applied Mechanics*, *18*(1), 31–38. https://doi.org/https://doi.org/10.1115/1.4010217

Moroglu, B., Uzuner, B. A., & Sadoglu, E. (2005). Behaviour of the model surface strip footing on reinforced sand.

Sadoglu, E., Cure, E., Moroglu, B., & Uzuner, B. A. (2009). Ultimate loads for eccentrically loaded model shallow strip footings on geotextile-reinforced sand. *Geotextiles and Geomembranes*, *27*(3), 176-182.

Sahu, R., Patra, C., Das, B., & Sivakugan, N. (2016). Ultimate bearing capacity of rectangular foundation on geogrid-reinforced sand under eccentric load. *International Journal of Geotechnical Engineering*, *10*(1), 52-56.

Shiau, J., Lyamin, A., & Sloan, S. (2003). Bearing capacity of a sand layer on clay by finite element limit analysis. *Canadian Geotechnical Journal*, *40*(5), 900-915.

Villard, P., Gourc, J.-P., & Blivet, J.-C. (2002). Prévention des risques d'effondrement de surface liés à la présence de cavités souterraines: une solution de renforcement par géosynthétique des remblais routiers et ferroviaires. *Revue française de géotechnique*(99), 23-34.

Wang, M., & Badie, A. (1985). Effect of underground void on foundation stability. *Journal of Geotechnical Engineering*, *111*(8), 1008-1019.

Wu, G., Zhao, M., Zhang, R., & Liang, G. (2020). Ultimate bearing capacity of eccentrically loaded strip footings above voids in rock masses. *Computers and Geotechnics*, *128*, 103819.

Wu, G., Zhao, M., Zhao, H., & Xiao, Y. (2020). Effect of eccentric load on the undrained bearing capacity of strip footings above voids. *International Journal of Geomechanics*, *20*(7), 04020078.